Blocking microglial pannexin-1 channels alleviates morphine withdrawal in rodents

Nicole E Burma[1,2], Robert P Bonin[3], Heather Leduc-Pessah[1,2], Corey Baimel[2], Zoe F Cairncross[1,2], Michael Mousseau[1,2], Jhenkruthi Vijaya Shankara[4], Patrick L Stemkowski[2], Dinara Baimoukhametova[2], Jaideep S Bains[2], Michael C Antle[2,4], Gerald W Zamponi[2], Catherine M Cahill[5], Stephanie L Borgland[2], Yves De Koninck[6] & Tuan Trang[1,2]

Opiates are essential for treating pain, but termination of opiate therapy can cause a debilitating withdrawal syndrome in chronic users. To alleviate or avoid the aversive symptoms of withdrawal, many of these individuals continue to use opiates[1–4]. Withdrawal is therefore a key determinant of opiate use in dependent individuals, yet its underlying mechanisms are poorly understood and effective therapies are lacking. Here, we identify the pannexin-1 (Panx1) channel as a therapeutic target in opiate withdrawal. We show that withdrawal from morphine induces long-term synaptic facilitation in lamina I and II neurons within the rodent spinal dorsal horn, a principal site of action for opiate analgesia. Genetic ablation of _Panx1_ in microglia abolished the spinal synaptic facilitation and ameliorated the sequelae of morphine withdrawal. Panx1 is unique in its permeability to molecules up to 1 kDa in size and its release of ATP[5,6]. We show that Panx1 activation drives ATP release from microglia during morphine withdrawal and that degrading endogenous spinal ATP by administering apyrase produces a reduction in withdrawal behaviors. Conversely, we found that pharmacological inhibition of ATP breakdown exacerbates withdrawal. Treatment with a Panx1-blocking peptide ([10]panx) or the clinically used broad-spectrum Panx1 blockers, mefloquine or probenecid, suppressed ATP release and reduced withdrawal severity. Our results demonstrate that Panx1-mediated ATP release from microglia is required for morphine withdrawal in rodents and that blocking Panx1 alleviates the severity of withdrawal without affecting opiate analgesia.

We investigated the mechanisms underlying opiate withdrawal by administering an opioid receptor antagonist (naloxone, 2 mg per kg body weight (mg/kg) intraperitoneally (i.p.)) to rats chronically treated for 5 d with systemic morphine sulfate (MS, **Supplementary Fig. 1a**). Naloxone administration precipitated a spectrum of autonomic and somatic withdrawal signs in morphine- but not saline-treated rats (**Supplementary Fig. 1b**), the overall severity of which was expressed as a cumulative withdrawal score (**Fig. 1a**). In morphine-treated rats, CD11b immunoreactivity was significantly elevated within the spinal dorsal horn, indicating that spinal microglia are activated by morphine treatment (**Fig. 1b** and **Supplementary Fig. 2**). Depletion of spinal lumbar microglia by intrathecal injections of a saporin (Sap)-conjugated antibody to Mac1 (Mac1–Sap; 20 µg) decreased withdrawal behaviors (**Supplementary Fig. 1b**) and attenuated the severity of withdrawal (**Fig. 1a**) without affecting morphine antinociception (**Fig. 1c**). By contrast, intrathecal injection of a nontargeting Sap (20 µg) control had no effect on spinal CD11b immunoreactivity (**Fig. 1b**) or naloxone-induced morphine withdrawal (**Supplementary Fig. 1b**).

In the central nervous system, Panx1 channels are expressed on neurons and glia[7,8]. Flow cytometric analysis of adult lumbar spinal cord homogenates revealed that morphine treatment resulted in elevated Panx1 expression on CD11b-positive cells (i.e., microglia) but not CD11b-negative cells (i.e., neurons and astrocytes) (**Fig. 1d** and **Supplementary Fig. 3**). We acutely isolated CD11b-positive cells from the spinal cord of morphine- or saline-treated rats and assessed Panx1 channel function by measuring BzATP-evoked uptake of YO-PRO-1 dye, an indicator of Panx1 channel activation[9,10]. YO-PRO-1 uptake was significantly greater in CD11b-positive cells isolated from morphine-treated rats (**Fig. 1e**). This response was blocked by [10]panx (10 µM)[5,11] but was not affected by a scrambled peptide ([scr]panx) (**Fig. 1e**). Both the increase in Panx1 protein expression (**Supplementary Fig. 4a**) and YO-PRO-1 uptake (**Fig. 1f**) were recapitulated in a BV-2 microglial-like cell line[12] exposed to morphine for 5 d _in vitro_. Dye uptake was further potentiated in the presence of naloxone (10 µM) (**Fig. 1f**) and blocked by [10]panx (10 µM) (**Fig. 1g**). Application of extracellular solution (ECS) as a vehicle control for BzATP did not evoke dye uptake (**Fig. 1f**). Moreover, treatment of cultured BV-2 cells with morphine and CTAP (a selective µ-receptor
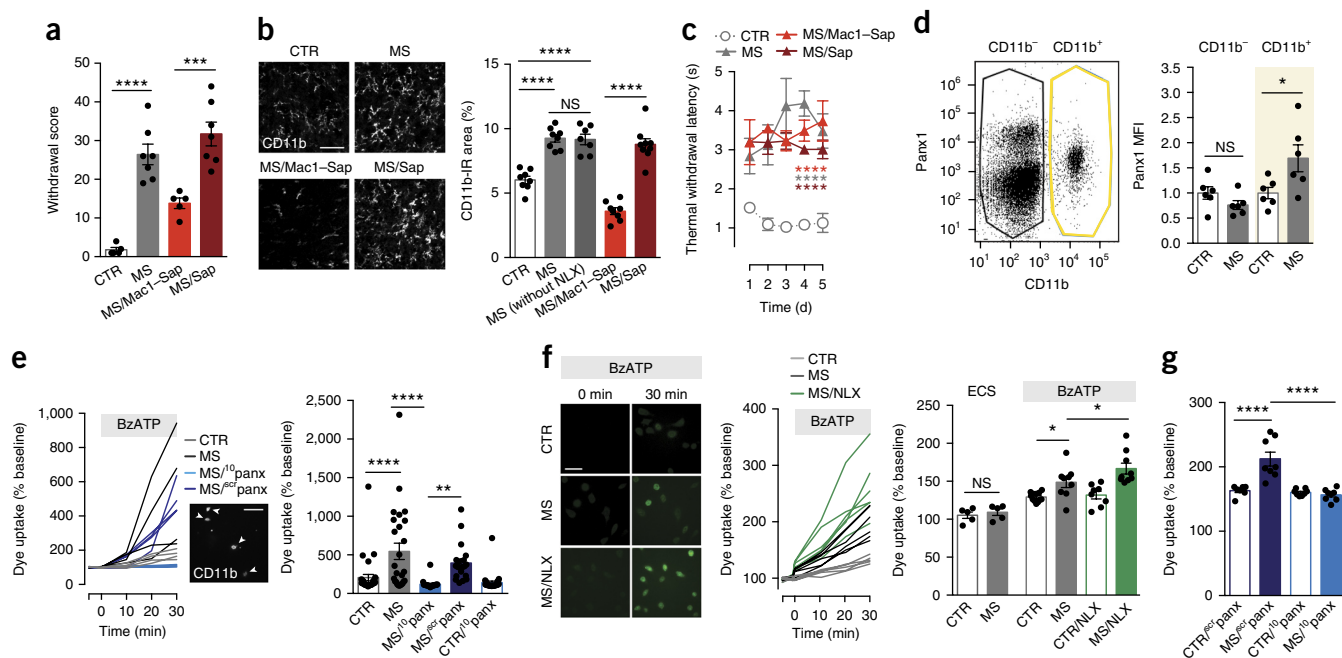
Figure 1 Repeated morphine treatment increases microglial Panx1 expression and activity. (**a**) Quantification of naloxone-induced composite behavioral withdrawal scores in rats treated for 5 d with saline (CTR, $n = 5$) or morphine sulfate (MS, $n = 7$), compared to MS-treated rats receiving intrathecal Mac1–Sap (MS/Mac1–Sap, $n = 5$) or Sap alone ($n = 7$). One-way ANOVA ($F_{3,20} = 27.95$) and Bonferroni *post hoc* test. (**b**) Representative images (left) and quantification (right) of CD11b immunoreactivity (IR) in spinal dorsal horn sections of rats treated with CTR or MS with or without naloxone (NLX), Mac1–Sap or Sap. $n = 7$–9 spinal cord sections analyzed. One-way ANOVA ($F_{4,35} = 50.96$) and Sidak *post hoc* test. (**c**) Quantification of MS-induced antinociception in the thermal tail flick test in rats treated with CTR or MS with or without Mac1–Sap or Sap over 5 d. $n = 4$ or 5 rats per group. Two-way repeated measures ANOVA (significant effect of treatment $F_{3,14} = 42.26$). (**d**) Left, flow cytometric analysis from control rat representing gating parameters for CD11b− (black) and CD11b+ (yellow) populations used to calculate mean fluorescence intensity (MFI) of Panx1 labeling. Right, quantification of Panx1 expression in CD11b− and CD11b+ spinal cord cell populations obtained from CTR- or MS-treated rats. MS MFI values are normalized to levels of control cells. $n = 6$ experimental replicates with 3 animals per group. One-way ANOVA ($F_{3,20} = 6.02$) and Sidak *post hoc* test. (**e**) Left, individual traces of BzATP-evoked YO-PRO-1 uptake in CD11b+ cultured spinal microglia from adult rats treated with CTR or MS in the presence or absence of [10]panx or [scr]panx. Inset, anti-CD11b staining to identify microglial cells (arrowheads) in the acutely isolated mixed culture preparation (Online Methods). Right, quantification of total dye uptake 30 min after BzATP application in CTR ($n = 32$ cells), MS ($n = 26$), MS/[10]panx ($n = 22$), MS/[scr]panx ($n = 20$) and CTR/[10]panx ($n = 29$) conditions. One-way ANOVA ($F_{5,146} = 9.89$) and Sidak *post hoc* test. (**f**) Representative images (left), individual traces (middle) and quantification at 30 min (right) of BzATP-evoked dye uptake in BV-2 cells treated for 5 d *in vitro* with CTR, MS or MS with NLX pretreatment (MS/NLX). ECS, control extracellular solution. $n = 5$ (ECS), 12 (BzATP CTR), 9 (MS and MS/NLX) or 8 (CTR/NLX) experiments per condition. One-way ANOVA ($F_{5,42} = 16.42$) with Sidak *post hoc* test. (**g**) Quantification of dye uptake in NLX-pre-treated BV-2 cells (CTR- or MS-treated) at 30 min after BzATP application in the presence of [scr]panx or [10]panx. $n = 7$ or 8 experiments per condition. ANOVA ($F_{3,27} = 19.02$). Error bars, s.e.m; each data point represents an individual animal or experiment. *P < 0.05, **P < 0.01, ***P < 0.001, ****P < 0.0001; NS, nonsignificant. Scale bars, 50 µm (**b**,**e**,**f**).

antagonist) together prevented the increase in Panx1 expression and function (**Supplementary Fig. 4a,c**), whereas repeated administration of the synthetic µ-receptor agonist peptide DAMGO mimicked the effects of morphine on Panx1 (**Supplementary Fig. 4b,d**).

The observation that naloxone potentiates Panx1 activity in morphine-treated microglia led us to examine whether microglial Panx1 channels might contribute to naloxone-induced morphine withdrawal behaviors. We tested this possibility by intrathecally administering [10]panx (10 µg) to morphine-treated rats 60 min before naloxone challenge and found significantly lower withdrawal scores than in morphine-treated rats injected with [scr]panx (**Fig. 2a**). To determine whether the requisite Panx1 is expressed on microglia, we created transgenic mice with a tamoxifen-dependent deletion of *Panx1* in cells expressing the chemokine C-X3-C motif receptor CX_3CR_1 (*Cx3cr1*-Cre[ERT2]::*Panx1*[flx/flx]). We confirmed in the lumbar spinal cord that the Cre[ERT2] reporter eYFP was localized to CD11b-positive cells (**Supplementary Fig. 5a**) and that there was a microglia-specific reduction in Panx1 expression in tamoxifen-treated *Cx3cr1*-Cre[ERT2]::*Panx1*[flx/flx] mice (**Supplementary Fig. 5b**). Performance

in the accelerating rotarod test was not altered in these microglial Panx1-deficient mice (**Supplementary Fig. 5c**). Spinal microglia isolated from adult microglial Panx1-deficient mice (7 d after tamoxifen injection in *Cx3cr1*-Cre[ERT2]::*Panx1*[flx/flx]) showed impaired YO-PRO-3 uptake (**Supplementary Fig. 5d**) but normal P2X7 receptor (P2X7R) function as measured by BzATP-evoked Ca^{2+} influx (**Supplementary Fig. 5e**). Morphine antinociception and morphine-induced spinal microglial reactivity remained notably intact in Panx1-deficient mice (**Fig. 2b,c**). However, when challenged with naloxone after morphine treatment, Panx1-deficient mice showed a significantly lower withdrawal score than morphine-treated Panx1-expressing mice (littermate vehicle-injected *Cx3cr1*-Cre[ERT2]::*Panx1*[flx/flx] mice) (**Fig. 2d** and **Supplementary Fig. 6**).

Cell turnover rates differ between central and peripheral CX_3CR_1-expressing populations[13]. Therefore, in another cohort of *Cx3cr1*-Cre[ERT2]::*Panx1*[flx/flx] mice, morphine injections were initiated 28 d after tamoxifen treatment to allow for repopulation of peripheral but not central CX_3CR_1-expressing cells. In this cohort of Panx1-deficient mice, the reduction in morphine withdrawal was comparable to that
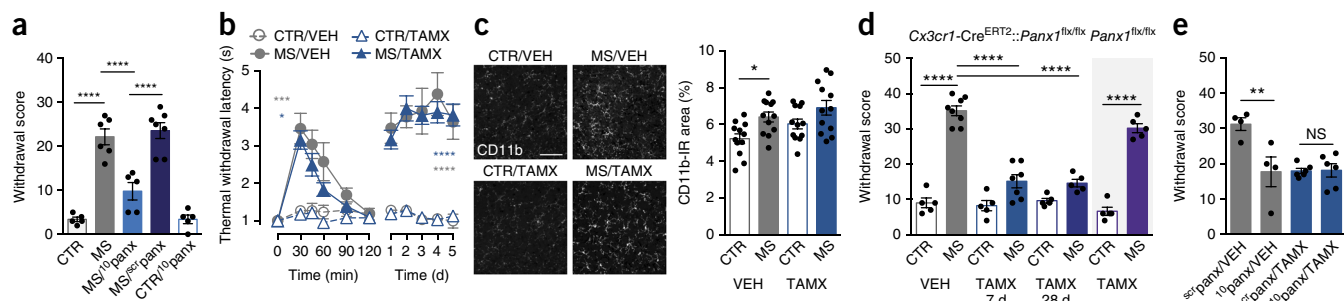
Figure 2 Blocking microglial Panx1 alleviates morphine withdrawal. (a) Effect of intrathecal [10]panx on naloxone-induced composite behavioral withdrawal scores in rats treated with morphine sulfate (MS) or saline (CTR) for 5 d. $n = 5–7$ rats per group. One-way ANOVA ($F_{4,23} = 38.29$) with Sidak *post hoc*. (b) Antinociception after a single MS injection (left) or over 5 d of MS treatment (right) in vehicle (VEH)- and tamoxifen (TAMX)-treated *Cx3cr1*-Cre[ERT2]::*Panx1*[flx/flx] mice assessed using the thermal tail immersion test. $n = 6$ mice (CTR/VEH, MS/VEH, CTR/TAMX) or 7 (MS/TAMX). Two-way repeated measures ANOVA (significant effect of time ($F_{5,105} = 40.19$), treatment ($F_{3,21} = 12.13$) and interaction ($F_{15,105} = 10.55$) for time course and significant effect of treatment ($F_{3,21} = 70.04$) for daily tail withdrawal latency). (c) Representative images (left) and quantification (right) of CD11b immunoreactivity (IR) in spinal dorsal horn sections of VEH- and TAMX-treated *Cx3cr1*-Cre[ERT2]::*Panx1*[flx/flx] mice after 5 d of MS or CTR treatment. Scale bar, 100 µm. $n = 12$ spinal cord sections per group. One-way ANOVA ($F_{3,44} = 5.38$) with Sidak *post hoc* test. (d) Naloxone-precipitated withdrawal scores in *Cx3cr1*-Cre[ERT2]::*Panx1*[flx/flx] mice treated with VEH or TAMX 7 or 28 d before MS withdrawal and in TAMX-treated *Panx1*[flx/flx] mice. One-way ANOVA ($F_{7,37} = 63.07$) with Sidak *post hoc*. $n = 5–8$ mice per group. (e) Naloxone-induced withdrawal scores in MS-treated VEH and TAMX *Cx3cr1*-Cre[ERT2]::*Panx1*[flx/flx] mice given intrathecal [scr]panx or [10]panx. $n = 4$ or 6 mice per group. One-way ANOVA ($F_{3,16} = 8.01$) with Sidak *post hoc*. Error bars, s.e.m; each data point represents an individual animal or experiment. *$P < 0.05$, **$P < 0.01$, ***$P < 0.001$, ****$P < 0.0001$; NS, nonsignificant.

observed in mice receiving morphine injections 7 d after tamoxifen treatment (**Fig. 2d**), suggesting that Panx1 on microglia, not peripheral CX$_3$CR$_1$-expressing cells, is required for morphine withdrawal. Furthermore, morphine withdrawal was attenuated in both male and female Panx1-deficient mice (**Supplementary Fig. 7**), indicating that microglial Panx1 critically contributes to opiate withdrawal in both sexes. As another control, we administered tamoxifen to mice lacking inducible Cre recombinase (*Panx1*[flx/flx]) and found that the severity of naloxone-precipitated withdrawal was indistinguishable from vehicle-treated Panx1-expressing mice (*Cx3cr1*-Cre[ERT2]::*Panx1*[flx/flx]) (**Fig. 2d**). Thus, tamoxifen *per se* does not affect morphine withdrawal. To further investigate the requirement for microglial Panx1 in morphine withdrawal, we compared the actions of [10]panx (10 µg) in Panx1-deficient and Panx1-expressing mice. We reasoned that if the effects of [10]panx were mediated by blocking Panx1 on microglia, they would be lost in the absence of microglial Panx1. Indeed, intrath-

ecal injection of [10]panx before naloxone challenge significantly attenuated morphine withdrawal in Panx1-expressing mice (**Fig. 2e**) but did not further ameliorate withdrawal in Panx1-deficient mice (**Fig. 2e**). This loss of [10]panx effect, together with the amelioration of withdrawal in Panx1-deficient mice, implicates microglial Panx1 in morphine withdrawal.

To investigate the mechanisms underlying Panx1-mediated withdrawal, we first measured spinal cFos expression as a cellular correlate of neuronal activation[14]. We determined that naloxone-precipitated withdrawal increased the number of cFos-positive neurons within the spinal dorsal horn of Panx1-expressing mice; this increase was suppressed in mice lacking microglial Panx1 (**Fig. 3a**). To assess neuronal function more directly, we used a whole lumbar spinal cord preparation with intact dorsal roots[15] prepared from Panx1-expressing or microglial Panx1-deficient adult mice that had been treated for 5 d with saline or morphine. We electrically stimulated the dorsal root to
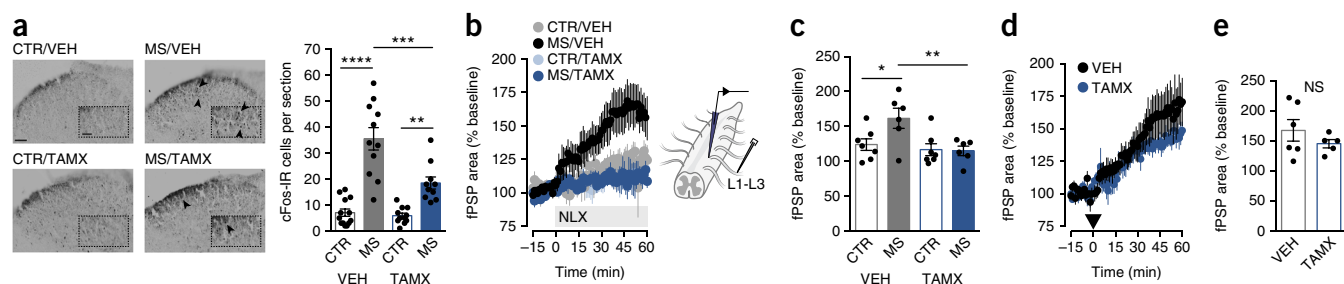

Figure 3 Genetic ablation of microglial Panx1 prevents naloxone-induced synaptic facilitation in spinal lamina I–II dorsal horn neurons of morphine-treated mice. (a) Representative images (left) and quantification (right) of cFos-immunoreactive (cFos-IR) neurons (arrowheads) in spinal dorsal horn (SDH) of vehicle (VEH)- and tamoxifen (TAMX)-treated *Cx3cr1*-Cre[ERT2]::*Panx1*[flx/flx] mice after 5 d of morphine sulfate (MS) or saline (CTR) treatment. Insets, magnified view of indicated cFos-IR neurons. Scale bars 50 µm (main) and 25 µm (inset). $n = 13$ (CTR/VEH), 11 (MS/VEH and CTR/TAMX) or 10 (MS/TAMX) spinal cords. One-way ANOVA ($F_{3,41} = 29.75$) with Sidak *post hoc*. (b) Left, fPSPs induced by naloxone (NLX) application in mice treated as in **a**. $n = 7$ (CTR/VEH and CTR/TAMX), 6 (MS/VEH) or 5 (MS/TAMX). Right, schematic of stimulation and recording setup for electrophysiology experiments. (c) Average fPSP area over the last 5 min of SDH recordings in mice as in **b**. $n = 6–7$. One-way ANOVA ($F_{3,22} = 4.73$) with Sidak *post hoc*. (d) Facilitation of fPSPs in lamina I–II of SDH after low-frequency electrical stimulation of dorsal roots (black arrowhead) in *Cx3cr1*-Cre[ERT2]::*Panx1*[flx/flx] mice treated with VEH ($n = 6$) or TAMX ($n = 5$). (e) Average fPSP area over last 5 min of electrical facilitation experiments in *Cx3cr1*-Cre[ERT2]::*Panx1*[flx/flx] mice. $n = 5–6$. Two-tailed *t*-test ($t = 1.062$, df = 9, $P = 0.32$). Error bars, s.e.m; each data point represents an individual animal or experiment. *$P < 0.05$, **$P < 0.01$, ***$P < 0.001$, ****$P < 0.0001$; NS, nonsignificant.
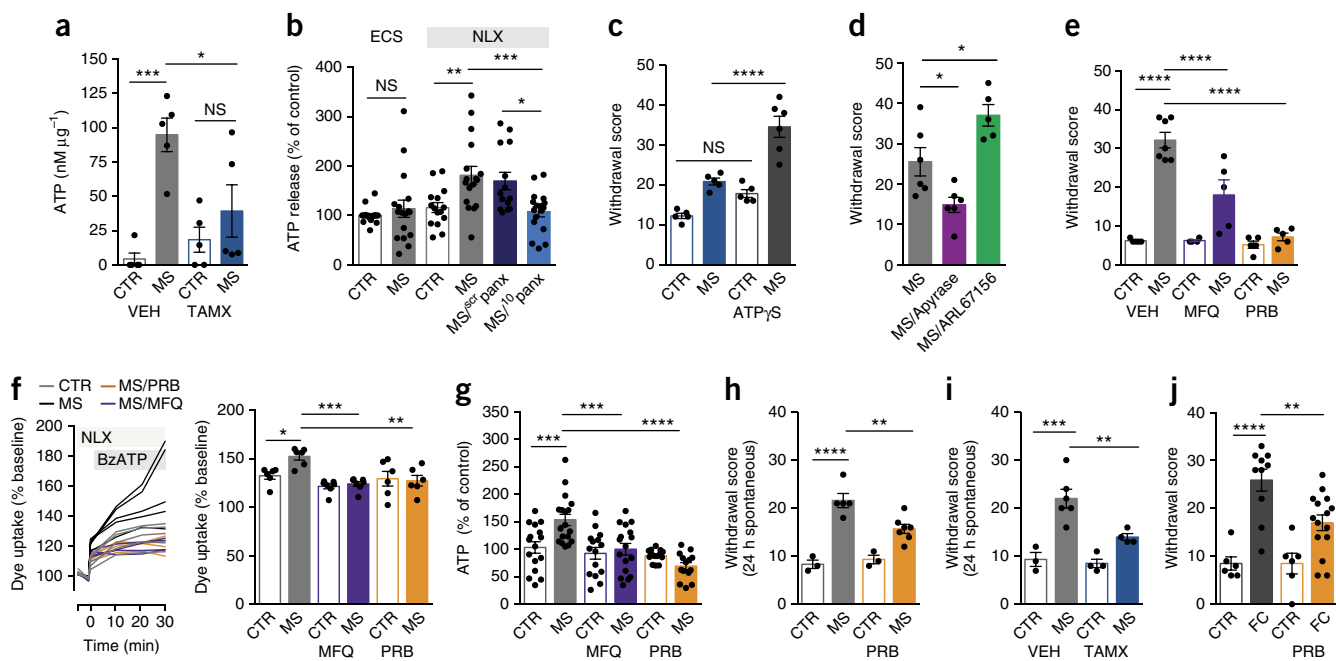
Figure 4 ATP released from microglial Panx1 is suppressed by mefloquine and probenecid. (**a**) Naloxone (NLX)-evoked ATP levels in artificial cerebral spinal fluid (aCSF) from lumbar spinal cord slices isolated from vehicle (VEH)- or tamoxifen (TAMX)-treated *Cx3cr1*-Cre^{ERT2}::*Panx1*$^{flx/flx}$ mice after 5 d of saline (CTR) or morphine (MS) treatment ($n = 5$ mice per treatment). One-way ANOVA ($F_{3,16} = 10.30$) with Sidak *post hoc*. (**b**) ATP levels in extracellular solution (ECS) supernatant from MS or CTR-treated BV-2 cells after application of ECS or NLX and ^{10}panx or ^{scr}panx. $n = 17$ (CTR/ECS, MS/ECS, MS/NLX, MS/^{10}panx), 15 (CTR/NLX) or 14 (MS/^{scr}panx) experiments. Data are relative to CTR-treated BV-2 cells exposed to ECS from the same experiment. One-way ANOVA ($F_{5,91} = 6.33$) with Sidak *post hoc*. (**c**) Effect of intrathecal ATPγS saline on composite withdrawal scores of TAMX-treated mice as in **a**. $n = 5$–6 mice per group. One-way ANOVA ($F_{3,17} = 34.04$) with Sidak *post hoc*. (**d**) NLX-precipitated withdrawal scores in MS-treated rats that received intrathecal saline (MS), apyrase (MS/Apyrase) or ARL67156 (MS/ARL67156). $n = 5$–6. One-way ANOVA ($F_{2,14} = 15.19$) with Bonferroni *post hoc*. (**e**) Effect of systemic injection of vehicle (VEH, $n = 5$ or 7), mefloquine (MFQ, $n = 4$ or 5) or probenecid (PRB, $n = 5$ per group) on NLX-precipitated withdrawal scores in rats that received CTR or MS for 5 d. One-way ANOVA ($F_{5,25} = 34.91$) with Sidak *post hoc*. (**f**) Individual traces (left) and quantification after 30 min (right) of BzATP-evoked YO-PRO-3 uptake in BV-2 cells treated for 5 d *in vitro* with CTR or MS in the presence or absence of MFQ or PRB. NLX was applied 10 min before baseline and was present in ECS throughout the experiment. $n = 6$ or 7 experiments. One-way ANOVA ($F_{5,32} = 6.12$) with Sidak *post hoc*. (**g**) ATP levels collected in ECS supernatant after NLX application in BV-2 cells treated for 5 d *in vitro* with CTR ($n = 16$ experiments) or MS ($n = 18$) alone or in the presence of MFQ ($n = 15$ (CTR) or 17 (MS)) or PRB ($n = 14$ per group). One-way ANOVA ($F_{7, 98} = 7.23$) with Sidak *post hoc*. (**h**) Spontaneous composite behavioral withdrawal scores in mice treated with saline (CTR, $n = 3$) or MS ($n = 5$) for 5 d, compared to mice that received systemic PRB ($n = 3$ or 7). One-way ANOVA ($F_{3,14} = 23.39$) with Sidak *post hoc*. (**i**) Quantification of spontaneous behavioral withdrawal scores in VEH- and TAMX-treated *Cx3cr1*-Cre^{ERT2}::*Panx1*$^{flx/flx}$ mice that received saline (CTR) or MS for 5 d. $n = 3$–6. One-way ANOVA ($F_{3,13} = 17.43$) with Sidak *post hoc*. (**j**) NLX-precipitated composite withdrawal scores in mice treated with saline ($n = 6$) or fentanyl citrate (FC, $n = 10$) for 7 d in the presence or absence of systemic PRB ($n = 6$ or 15). One-way ANOVA ($F_{3,33} = 14.87$) with Sidak *post hoc*. Error bars, s.e.m; each data point represents an individual animal or experiment. *$P < 0.05$, **$P < 0.01$, ***$P < 0.001$, ****$P < 0.0001$; NS, nonsignificant.

evoke postsynaptic field potentials (fPSPs) recorded from laminae I–II of the spinal dorsal horn and found that bath application of naloxone (10 μM) produced a slow-rising facilitation of fPSPs that persisted for at least 60 min in morphine- but not saline-treated Panx1-expressing mice (**Fig. 3b,c**). By contrast, this response to naloxone did not occur in morphine-treated Panx1-deficient mice (**Fig. 3b,c**). The absence of synaptic facilitation in these mutant mice was not due to a general defect in spinal synaptic facilitation, because electrically stimulating the dorsal roots of Panx1-deficient mice at low frequency (2 Hz) produced a robust and long-lasting increase in fPSPs (**Fig. 3d,e**).

Because ATP release is a key consequence of Panx1 activation[6,16], we asked whether Panx1-mediated ATP release occurs during withdrawal. To test this, we bath-applied naloxone (10 μM) to spinal cord slices isolated from Panx1-expressing and Panx1-deficient mice that had been treated for 5 d with saline or morphine. We measured the amount of ATP in spinal superfusates and found that the level of ATP in response to naloxone was significantly higher in morphine- than in saline-treated Panx1-expressing mice (**Fig. 4a**). Naloxone-induced ATP release was not observed in slices prepared

from Panx1-deficient mice (**Fig. 4a**). To test whether ATP is directly released from microglia, we applied naloxone to microglia in culture. Supernatants of morphine-treated microglia showed increase in ATP, and this increase was blocked by ^{10}panx (**Fig. 4b**). Thus, naloxone induces the release of ATP from morphine-treated microglia via a Panx1-dependent mechanism.

To test whether ATP contributes to morphine withdrawal, we administered ATPγS (100 μM) intrathecally to Panx1-deficient mice, which display attenuated morphine withdrawal behaviors. In these mice, local delivery of the ATP analog together with naloxone challenge restored a spectrum of withdrawal behaviors; these behaviors were not observed when ATPγS was administered to saline-treated Panx1-deficient mice (**Fig. 4c**). We reasoned that if ATP is required for morphine withdrawal, then altering endogenously released ATP in the spinal cord might influence withdrawal behaviors. In morphine-treated rats, we tested this possibility by intrathecal administration of the ATP-degrading enzyme apyrase (10 units)[17], which produced a notable reduction in withdrawal score (**Fig. 4d**). Conversely, inhibiting ATP breakdown by intrathecally administering

the ecto-ATPase inhibitor ARL67156 (10 nmol)[18,19] exacerbated morphine withdrawal (**Fig. 4d**). We therefore conclude that ATP is a key substrate for morphine withdrawal.

P2X7R activation is a core mechanism for opening Panx1 channels[5,10]. We determined that P2X7R expression was selectively increased in spinal microglia isolated from morphine-dependent rats (**Supplementary Fig. 8a**), and blockade of these receptors by intrathecal administration of the selective P2X7R antagonist A-740003 attenuated withdrawal (**Supplementary Fig. 8b**). These findings position P2X7R as an upstream signaling node through which morphine potentiates Panx1 function, defining P2X7R–Panx1 as a microglial signaling ensemble required for morphine withdrawal. Specifically targeting Panx1 while leaving P2X7R function intact could, however, be the preferred strategy for treating opiate withdrawal.

Having established that Panx1 is crucially involved in morphine withdrawal, we tested as proof of concept two clinically used broad-spectrum Panx1 inhibitors: probenecid, an anti-gout medication[20], and mefloquine, an antimalarial drug[21]. In morphine-treated rats, systemic administration of probenecid or mefloquine 60 min before naloxone challenge significantly ameliorated morphine withdrawal (**Fig. 4e** and **Supplementary Fig. 9a**). These compounds also blocked BzATP-evoked potentiation of Panx1 activation (**Fig. 4f** and **Supplementary Fig. 9b**) and suppressed ATP release in morphine-treated microglia cultures (**Fig. 4g** and **Supplementary Fig. 9c**) without altering P2X7R-mediated calcium responses (**Supplementary Fig. 10a,b**).

To further extend the potential clinical utility of probenecid, we tested the actions of this compound in a model of spontaneous morphine withdrawal that does not rely on naloxone challenge. Mice given a 5-d morphine treatment showed robust withdrawal behaviors 24 h after morphine cessation, and these behaviors were attenuated by a systemic injection of probenecid (50 mg/kg, i.p.) (**Fig. 4h**). Spontaneous withdrawal was also reduced in Panx1-deficient mice (**Fig. 4i**), suggesting a common microglial Panx1-dependent mechanism in both naloxone-precipitated and spontaneous withdrawal. Finally, we investigated the effects of probenecid on fentanyl, another clinically used and widely abused opioid. In fentanyl-treated mice, naloxone precipitated robust withdrawal that was ameliorated by probenecid (**Fig. 4j**). Taken together, the effects of probenecid and mefloquine in alleviating opiate withdrawal open the possibility that these, and other clinically available broad-spectrum Panx1 inhibitors, have potential application in the treatment of opiate withdrawal.

In summary, we have discovered that a substrate within the spinal cord—microglial Panx1-mediated ATP release—underlies the cellular and behavioral correlates of morphine withdrawal. We propose that Panx1 activation is a fundamental mechanism through which microglia cause long-term synaptic facilitation in spinal lamina I–II neurons during withdrawal. This form of neuronal hyperexcitability is a cardinal feature of withdrawal[14,22], and we demonstrate here that this central tenet of withdrawal occurs directly in the spinal cord of morphine-treated animals. Because opiate withdrawal engages both spinal and supraspinal mechanisms, including the periaqueductal gray[14], locus coeruleus[23], ventral tegmental area[24–26] and nucleus accumbens[27], descending inputs from these supraspinal regions may influence spinal facilitation in the intact system. However, our isolated spinal cord preparation suggests that intrinsic spinal mechanisms are sufficient for synaptic facilitation during withdrawal, and as further evidence for a spinal locus of opiate action, we show that spinal manipulations targeting Panx1 channels or ATP levels effectively block or recapitulate the behavioral and cellular corollaries of withdrawal. Although we do not rule out contributions from supraspinal

mechanisms, the potent alleviation of opiate withdrawal by clinically used Panx1-blocking drugs (probenecid and mefloquine) highlights the potential of our findings for immediate therapeutic translation. Targeting Panx1 channels may therefore represent a new clinical strategy for alleviating withdrawal symptoms without impairing morphine analgesia.

METHODS

Methods, including statements of data availability and any associated accession codes and references, are available in the online version of the paper.

Note: Any Supplementary Information and Source Data files are available in the online version of the paper.

AUTHOR CONTRIBUTIONS
N.E.B. and T.T. conceived and designed the project. N.E.B., R.P.B., H.L.-P., C.B., Z.F.C., M.M., J.V.S., P.L.S., D.B. and C.M.C. performed the experiments. T.T., Y.D.K., S.L.B., M.C.A., G.W.Z. and J.S.B. supervised the experiments. N.E.B., R.P.B., H.L.-P., M.C.A. and C.M.C. analyzed the data. N.E.B. and T.T. wrote the manuscript. All authors read and approved the manuscript.

COMPETING FINANCIAL INTERSTS
The authors declare no competing financial interests.

Reprints and permissions information is available online at http://www.nature.com/reprints/index.html.

1. Stotts, A.L. *et al.* A stage I pilot study of acceptance and commitment therapy for methadone detoxification. *Drug Alcohol Depend.* **125**, 215–222 (2012).
2. Weiss, R.D. *et al.* Reasons for opioid use among patients with dependence on prescription opioids: the role of chronic pain. *J. Subst. Abuse Treat.* **47**, 140–145 (2014).
3. Frank, J.W. *et al.* Patients' perspectives on tapering of chronic opioid therapy: a qualitative study. *Pain Med.* **17**, 1838–1847 (2016).
4. Yarborough, B.J.H. *et al.* Methadone, buprenorphine and preferences for opioid agonist treatment: a qualitative analysis. *Drug Alcohol Depend.* **160**, 112–118 (2016).
5. Pelegrin, P. & Surprenant, A. Pannexin-1 mediates large pore formation and interleukin-1β release by the ATP-gated P2X7 receptor. *EMBO J.* **25**, 5071–5082 (2006).
6. Sandilos, J.K. *et al.* Pannexin 1, an ATP release channel, is activated by caspase cleavage of its pore-associated C-terminal autoinhibitory region. *J. Biol. Chem.* **287**, 11303–11311 (2012).
7. Huang, Y., Grinspan, J.B., Abrams, C.K. & Scherer, S.S. Pannexin1 is expressed by neurons and glia but does not form functional gap junctions. *Glia* **55**, 46–56 (2007).
8. Iglesias, R., Dahl, G., Qiu, F., Spray, D.C. & Scemes, E. Pannexin 1: the molecular substrate of astrocyte "hemichannels". *J. Neurosci.* **29**, 7092–7097 (2009).
9. Iglesias, R. *et al.* P2X7 receptor–pannexin1 complex: pharmacology and signaling. *Am. J. Physiol. Cell Physiol.* **295**, C752–C760 (2008).
10. Sorge, R.E. *et al.* Genetically determined P2X7 receptor pore formation regulates variability in chronic pain sensitivity. *Nat. Med.* **18**, 595–599 (2012).
11. Thompson, R.J. *et al.* Activation of pannexin-1 hemichannels augments aberrant bursting in the hippocampus. *Science* **322**, 1555–1559 (2008).
12. Masuda, T. *et al.* Transcription factor IRF5 drives P2X4R+-reactive microglia gating neuropathic pain. *Nat. Commun.* **5**, 3771 (2014).
13. Parkhurst, C.N. *et al.* Microglia promote learning-dependent synapse formation through brain-derived neurotrophic factor. *Cell* **155**, 1596–1609 (2013).

14. Bagley, E.E. *et al.* Drug-induced GABA transporter currents enhance GABA release to induce opioid withdrawal behaviors. *Nat. Neurosci.* **14**, 1548–1554 (2011).
15. Bonin, R.P. & De Koninck, Y. A spinal analog of memory reconsolidation enables reversal of hyperalgesia. *Nat. Neurosci.* **17**, 1043–1045 (2014).
16. Huang, Y.-J. *et al.* The role of pannexin 1 hemichannels in ATP release and cell–cell communication in mouse taste buds. *Proc. Natl. Acad. Sci. USA* **104**, 6436–6441 (2007).
17. Chiang, C.Y. *et al.* Endogenous ATP involvement in mustard-oil-induced central sensitization in trigeminal subnucleus caudalis (medullary dorsal horn). *J. Neurophysiol.* **94**, 1751–1760 (2005).
18. Beckel, J.M. *et al.* Pannexin 1 channels mediate the release of ATP into the lumen of the rat urinary bladder. *J. Physiol. (Lond.)* **593**, 1857–1871 (2015).
19. Nakatsuka, T. & Gu, J.G. ATP P2X receptor–mediated enhancement of glutamate release and evoked EPSCs in dorsal horn neurons of the rat spinal cord. *J. Neurosci.* **21**, 6522–6531 (2001).
20. Silverman, W., Locovei, S. & Dahl, G. Probenecid, a gout remedy, inhibits pannexin 1 channels. *Am. J. Physiol. Cell Physiol.* **295**, C761–C767 (2008).
21. Iglesias, R., Spray, D.C. & Scemes, E. Mefloquine blockade of pannexin1 currents: resolution of a conflict. *Cell Commun. Adhes.* **16**, 131–137 (2009).
22. Drdla, R., Gassner, M., Gingl, E. & Sandkühler, J. Induction of synaptic long-term potentiation after opioid withdrawal. *Science* **325**, 207–210 (2009).
23. Han, M.-H. *et al.* Role of cAMP response element–binding protein in the rat locus ceruleus: regulation of neuronal activity and opiate withdrawal behaviors. *J. Neurosci.* **26**, 4624–4629 (2006).
24. Koo, J.W. *et al.* Epigenetic basis of opiate suppression of *Bdnf* gene expression in the ventral tegmental area. *Nat. Neurosci.* **18**, 415–422 (2015).
25. Vargas-Perez, H. *et al.* Ventral tegmental area BDNF induces an opiate-dependent-like reward state in naive rats. *Science* **324**, 1732–1734 (2009).
26. Laviolette, S.R., Gallegos, R.A., Henriksen, S.J. & van der Kooy, D. Opiate state controls bi-directional reward signaling via GABAA receptors in the ventral tegmental area. *Nat. Neurosci.* **7**, 160–169 (2004).
27. Zhu, Y., Wienecke, C.F.R., Nachtrab, G. & Chen, X. A thalamic input to the nucleus accumbens mediates opiate dependence. *Nature* **530**, 219–222 (2016).

ONLINE METHODS

Animals. Adult male rats and mice were used (rats aged 7–8 weeks; mice aged 8–12 weeks for behavioral experiments and 6–10 weeks for electrophysiology experiments). Mice and rats were housed under a 12-h/12-h light/dark cycle with *ad libitum* access to food and water and were randomly allocated to different test groups. All experiments were approved by the University of Calgary, Université Laval and University of California Irvine Animal Care Committees and are in accordance with the guidelines of the Canadian Council on Animal Care and the US National Institutes of Health Guide for the Care of Use of Laboratory Animals.

Morphine dosing paradigm and nociceptive behavioral models. Morphine sulfate (PCCA) prepared in 0.9% sterile saline solution was injected i.p. twice daily (8 a.m. and 5 p.m.) into male Sprague-Dawley rats (weight ranging 200–250 g, escalating doses from 10 to 45 mg/kg)[28], C57BL/6 mice, male and female *Cx3cr1*-Cre[ERT2]::*Panx1*[flx/flx] or *Panx1*[flx/flx] mice (weight ranging 16–30 g, escalating doses from 7.5 to 50 mg/kg). Thermal nociceptive thresholds were assessed using the tail-flick test (rats) and the tail-immersion test (mice). For rats, an infrared thermal stimulus (Ugo Basile) was applied to the ventral surface of the tail, and time latency for tail removal from the stimulus was recorded. For mice, the distal portion of the tail was submerged in a 50 °C water bath, and time latency for tail removal from the stimulus was recorded. A maximum cutoff time was set at 10 s to prevent tissue damage. Nociceptive measurements were taken before and 30 min after morphine injections, and values were normalized to daily baseline. In a subset of mouse experiments, a time course of morphine-induced antinociception was performed at 30, 45, 60, 90 and 120 min after a single acute injection of morphine (7.5 mg/kg).

Behavioral assessment of morphine withdrawal. Rats and mice received ascending doses of morphine i.p. at 8-h intervals (rats: day 1, 10 mg/kg; day 2, 20 mg/kg; day 3, 30 mg/kg; day 4, 40 mg/kg; mice: day 1, 7.5 and 15 mg/kg; day 2, 20 and 25 mg/kg; day 3, 30 and 35 mg/kg; day 4, 40 and 45 mg/kg). On day 5, rats and mice received a morning injection of morphine (rats, 45 mg/kg; mice, 50 mg/kg) and 2 h later naloxone (2 mg/kg, naloxone hydrochloride dihydrate, Sigma) to rapidly induce opiate withdrawal. Control rats and mice received equivalent volumes of 0.9% saline and were challenged with naloxone on day 5. Signs of withdrawal were recorded as previously described[29]. Jumping, teeth chattering, wet-dog shakes, headshakes and grooming behaviors were evaluated at 5-min intervals for a total test period of 30 min, and a standardized score of 0 to 3 was assigned to each behavior. Allodynia, piloerection, salivation, ejaculation and tremors or twitching were also evaluated, with 1 point given to the presence of the behavior during each 5-min interval. All signs were counted and compiled to yield a cumulative withdrawal score. Rats and mice were weighed before and after naloxone challenge to calculate weight loss. In all behavioral studies, experimenters were blind to the drug treatment group and genetic profile of rats and mice. In a subset of experiments, spontaneous withdrawal behaviors were assessed in mice 24 h after last morphine or control injection (on day 6).

Intrathecal drug administration. In a subset of experiments, rats and mice were subject to drug administration by intrathecal injection under 2% isoflurane (vol/vol) by lumbar puncture method as previously described[30]. Mac1–Sap or Sap (20 μg, Advanced Targeting Systems) was injected on days 1 and 3 before morning morphine injections. Intrathecal injections of [10]panx (10 μg, WRQAAFVDSY, New England Peptide), [scr]panx (10 μg, FSVYWAQADR, New England Peptide) and A-740003 (10 μL of 10 μM, Sigma) were delivered 60 min before naloxone-precipitated withdrawal, and intrathecal apyrase (10 units, Sigma) and ARL67156 (10 nmol, Sigma) were delivered 15 min before naloxone. ATPγS (100 μM, Roche) was delivered intrathecally immediately before naloxone-precipitated withdrawal without the use of isoflurane. All control animals received an equivalent volume of intrathecal 0.9% sterile saline on a timeline identical to that used for treated animals from the same experiment.

Systemic drug administration. Morphine-dependent rats received systemic mefloquine (45 mg/kg i.p., Sigma; or 20 mg/kg i.p., Bioblocks) or probenecid (50 mg/kg i.p., Sigma) 60 min before naloxone-precipitated withdrawal. In the spontaneous withdrawal experiments, mice received probenecid (50 mg/kg i.p., Sigma) 23 h after the last morphine or control injection (60 min before assessment of spontaneous withdrawal) on day 6. In the fentanyl withdrawal experiments, mice received probenecid (50 mg/kg i.p., Sigma) 10 min after last fentanyl injection and 20 min before naloxone-precipitated withdrawal on day 7. Both mefloquine and probenecid were reconstituted in β-cyclodextrin (Sigma), and control animals received systemic β-cyclodextrin.

Assessment of sensorimotor coordination. Sensorimotor coordination was evaluated using the accelerating rotarod test (Panlab, Harvard Apparatus). All mice underwent two conditioning trials before testing. Motor behavior was analyzed 7 d after last tamoxifen or vehicle injection. In brief, mice were placed on a rotating rod set to gradually accelerate from 4 to 40 r.p.m. over 5 min. The trial was terminated when the mouse fell off the apparatus, and both time and terminal speed (r.p.m.) were recorded.

Behavioral assessment of fentanyl withdrawal. Fentanyl citrate (West Ward Pharmaceuticals) prepared in 0.9% sterile saline solution was injected i.p. at ascending doses (day 1, 5 and 25 μg/kg at 8-h intervals; day 2, 50 μg/kg at 8-h intervals; day 3, 75 μg/kg at 8-h intervals; day 4, 100 μg/kg at 8-h intervals; day 5, 150 μg/kg at 8-h intervals; day 6 150 μg/kg at 4-h intervals). On day 7, mice received two injections of fentanyl 4 h apart (150 μg/kg) and 30 min after the second dose naloxone (10 mg/kg, Sigma) to rapidly induce opiate withdrawal. Control mice received an equivalent volume of 0.9% saline and were challenged with naloxone on day 7. Signs of withdrawal were recorded after naloxone injection for a 20-min test period as described above for morphine withdrawal. The experimenter was blind to the drug treatment groups of the mice.

Western blotting. Cultured microglia were harvested in 150 μL lysis buffer containing 50 mM Tris-HCl, 150 mM NaCl, 10 mM EDTA, 0.1% Triton-X, and 5% glycerol. Lysis buffer contained protease inhibitors (Sigma) and phosphatase inhibitors (GBiosciences). Total protein was measured using a Pierce BCA Protein Assay Kit (Thermo Scientific). Samples were heated at 95 °C for 5 min in loading buffer (350 mM Tris, 30% glycerol, 1.6% SDS, 1.2% bromophenol blue, 6% β-mercaptoethanol) then electrophoresed on a pre-cast SDS gel (4–12% Tris-HCl, Bio-Rad) and transferred onto a nitrocellulose membrane. After blocking, membranes were incubated with rabbit antibody to Panx1 (1:250, Life Technologies, 488100) and mouse antibody to β-actin (1:2,000, Sigma-Aldrich, A5316). Membranes were washed and incubated for 2 h at room temperature in fluorophore-conjugated secondary antibodies (anti-rabbit- and anti-mouse-conjugated immunoreactivity (IR) dyes 1:5,000, Mandel Scientific) and quantified by direct detection of secondary antibody fluorescence at 680 and 800 nm (LICOR Odyssey CLx). Band intensity was quantified using ImageJ, normalized to β-actin and expressed relatively to control samples.

Isolation of adult mixed neuron–glia culture. Rats and mice were anaesthetized and perfused transcardially with PBS. Spinal cord and (for mice only) brain tissues were isolated and placed in HBSS. After blunt dissociation, spinal cord contents were filtered through a 70 μm cell strainer into DMEM containing 10 mM HEPES and 5% FBS. Isotonic Percoll (density 1.23 g/mL) was added to the cell suspension, followed by a 1.08 g per mL Percoll underlay[31]. Samples were spun at 3,000 r.p.m. for 30 min at 20 °C. Following centrifugation, myelin debris was removed, and the interface between Percoll gradients was collected and transferred into fresh medium. Samples were centrifuged again at 1,350 r.p.m. for 10 min at 4 °C, and the pellet was reconstituted in PBS containing 10% FBS (for flow cytometry) or DMEM containing 10% FBS and 1% penicillin–streptomycin (for live-cell imaging).

Flow cytometry. Mixed neuron–glia culture was isolated from adult rat spinal cord as described above. Cells were stained with fluorophore-conjugated CD11b/c–PE (1:500 eBioscience, 12-0110-82) and either rabbit antibody to Panx1 (1:400 Pierce, PA5-34475, and 1:400 Life Technologies) preincubated with fluorophore-conjugated anti-rabbit secondary antibody or fluorophore-conjugated P2X7R–ATTO 633 (1:250 Alomone, APR-008-FR) for 1 h at 20 °C.

Cell fluorescence was measured by an Attune Acoustic Focusing Cytometer (Applied Biosystems). Live single-cell population was gated using forward and side scatter plots. CD11b- and Panx1-positive staining were gated using BL2 and RL1 intensities, respectively, in single stained cells compared to unstained cells.

BV-2 microglia culture. BV-2 microglial-like cells were provided by M. Tsuda and K. Biber[12]. Cells were maintained in DMEM (Gibco) containing 5% FBS and 1% penicillin–streptomycin (Pen-Strep) at 37°C with 5% CO_2 and treated with morphine (10 µM), morphine and CTAP (1 µM), DAMGO (1 µM), saline and CTAP, or saline once a day for 5 d. BV-2 microglial-like cells were found to be free of mycoplasma contamination using MycoFluor Mycoplasma Detection Kit (Molecular Probes).

Calcium imaging. Cells were incubated for 30 min with the fluorescent Ca^{2+} indicator dye Fura-2 a.m. (2.5 µM, Molecular Probes) in extracellular solution (ECS) containing 140 mM NaCl, 5.4 mM KCl, 1.3 mM $CaCl_2$, 10 mM HEPES and 33 mM glucose (pH 7.35, 315 mOsm)[32]. In a subset of experiments, mefloquine (40 µM, Sigma or 100 nM, Bioblocks) or probenecid (1 mM, Life Technologies) were bath applied in ECS after loading of Fura-2 a.m. and incubated at room temperature for 30 min before BzATP (100 µM) stimulation. All experiments were conducted at room temperature using an inverted microscope (Nikon Eclipse Ti C1SI Spectral Confocal), and the fluorescence of individual microglia was recorded using EasyRatioPro software (PTI). Excitation light was generated from a xenon arc lamp and passed alternately through 340- or 380-nm band-pass filters (Omega Optical). The 340/380 fluorescence ratio was calculated after baseline subtraction.

Generation of *Cx3cr1*-Cre[ERT2]::*Panx1*[flx/flx] mice. Mice with microglial-specific deletion of *Panx1* were generated using a Cre-*loxP* system. *Panx1*[flx/flx] homozygote mice[33] containing *loxP* sequences flanking exon 2 of the *Panx1* gene were crossed with C57BL6/J mice expressing Cre-ERT2 fusion protein and enhanced yellow fluorescent protein (eYFP) under the *Cx3cr1* promoter (Jax mice: B6.129P2(Cg)-Cx3cr1[tm2.1(cre/ERT)Litt]/WganJ, stock number 021160). Progeny genotype was screened by PCR, and homozygous *Panx1*[flx/flx] and *Cx3cr1*-Cre[ERT2] mice were bred and backcrossed for 8 generations to yield the conditional knockout *Cx3cr1*-Cre[ERT2]::*Panx1*[flx/flx] mice. To induce Cre recombination, mice were injected i.p. with 1 mg per day tamoxifen (Sigma) for 5 d. Control mice were littermates that received vehicle injections (sunflower oil with 10% ethanol) for 5 d, while tamoxifen-related effects were controlled for using *Panx1*[flx/flx] littermate mice that received 5 d of tamoxifen injections. In the majority of experiments, testing occurred 7 d after final tamoxifen injection. In a subset of experiments, behavioral assessment of morphine withdrawal was conducted 28 d after final tamoxifen injection to control for effects of peripheral Cx3cr1-expressing cells.

YO-PRO dye uptake. After 5 d of morphine or saline treatment, cell culture medium was removed, and the BV-2 cells were incubated in ECS containing either YO-PRO-1 or YO-PRO-3 dye (2.5 µM, Invitrogen). After a 5-min baseline recording, cells were stimulated with BzATP (150 µM, Sigma), and dye uptake was recorded for 30 min. Cell viability was assessed immediately after 30 min recording by application of ionomycin (1 µM, Sigma). Cells that did not respond to ionomycin were excluded from the analysis. YO-PRO-1 dye fluorescence emission (491/509 nm) or YO-PRO-3 dye fluorescent emission (612/631 nm) was detected at 37 °C using a FilterMax F5 plate reader (Molecular Devices). Drugs used included [10]panx (10 µM, New England Peptide), [scr]panx (10 µM, New England Peptide), naloxone (10 µM, Sigma), probenecid (1 mM, Life Technologies), and mefloquine (40 µM, Sigma or 100 nM, Bioblocks). Drugs were bath applied in ECS containing YO-PRO-1 dye (in the absence of morphine) and incubated at 37 °C for 10 min before BzATP stimulation. For the BV-2 cell experiments, fluorescence emission at 30 min after BzATP application was calculated as an average of the entire imaging field as percentage change from baseline, and responses at 30 min were averaged over multiple independent experiments. Representative images of BV-2 YO-PRO-1 dye uptake were taken using EasyRatioPro software (PTI) at room temperature using an inverted microscope (Nikon Eclipse Ti C1S1 Spectral Confocal). Individual traces of BV-2 YO-PRO-1 dye uptake were

taken at 10-min intervals and represent the average response of all BV-2 cells in the recorded view from a subset of experiments. To assess Panx1 function in adult microglia, neuron–glia mixture culture was isolated from adult Sprague-Dawley rats treated with saline or morphine for 5 d, or from *Cx3cr1*-Cre[ERT2]::*Panx1*[flx/flx] mice treated with tamoxifen or vehicle for 5 d as described above. Once isolated, cells were plated in DMEM containing 10% FBS and 1% Pen-Strep and incubated overnight at 37 °C with 5% CO_2. Cells were washed and incubated with DAPI (1:10,000) for 10 min, and then incubated in YO-PRO-1 dye (rats) or YO-PRO-3 dye (mice). In rats, microglia were identified from mixed adult neuronal–glial culture using a fluorophore-conjugated antibody CD11b/c-PE (1:500, eBioscience), and in mice microglia were identified by endogenous expression of eYFP. Fluorescence of individual microglia were recorded for a 5-min baseline period and then for 30 min after BzATP stimulation (300 µM). Individual traces were taken at 10-min intervals and represent responses from a subset of individual microglia. Fluorescence emission at 30 min was expressed as percentage change from the baseline recorded from the same cell.

Naloxone-induced ATP release. ATP levels were detected using bioluminescence by combining samples with recombinant firefly luciferase and its substrate D-luciferin (ATP Determination Kit, Life Technologies). The ATPase inhibitor (ARL67156, 1 µM, Sigma) was added to the ECS or aCSF (in mM: 126 NaCl, 1.6 KCl, 1.1 NaH_2PO_4, 1.4 $MgCl_2$, 2.4 $CaCl_2$, 26 $NaHCO_3$, 11 glucose) to minimize breakdown of ATP, and samples were incubated in medium for 30 min before naloxone challenge to reduce mechanically induced ATP release. Samples were exposed to naloxone (10 µM) for 30 min, then the supernatant was collected and samples read immediately using a FilterMax F5 plate reader at 28 °C. For experiments with BV-2 microglial-like cultures, cells were incubated in [10]panx (10 µM, New England Peptide), [scr]panx (10 µM, New England Peptide), probenecid (1 mM, Life Technologies), mefloquine (40 µM, Sigma or 100 nM, Bioblocks) or ECS for 10 min before naloxone exposure. Final ATP measurement was expressed relatively to control samples (saline-treated BV-2 cells exposed to ECS) from the same plate. For ATP release in spinal cord slices, tamoxifen- or vehicle-treated *Cx3cr1*-Cre[ERT2]::*Panx1*[flx/flx] mice were perfused with ice-cold oxygenated sucrose-substituted aCSF (s-aCSF in mM: 252 sucrose, 2.5 KCl, 1.5 $CaCl_2$, 6 $MgCl_2$, 10 D-glucose), and the spinal cord rapidly dissected. The lumbar segment of the spinal cord was sliced into 300 µm sections, and incubated in oxygenated 32 °C aCSF for 1 h. Spinal cord slices were then transferred to room temperature oxygenated aCSF and exposed to naloxone (10 µM). For quantification, ATP release was normalized to total protein of each sample.

Histological procedures. Rats and mice were anesthetized with pentobarbital (Bimeda-MTC Animal Health Inc.) and perfused transcardially with 4% paraformaldehyde (PFA) (wt/vol). Following dissection, the spinal lumbar segment was post-fixed in 4% PFA, then cryoprotected in 30% sucrose. Spinal cords were sliced at 30 µm into free-floating sections, then incubated overnight at 4 °C in mouse antibody to CD11b (1:50, CBL1512 EMD Milipore), rat antibody to CD11b (1:250, Abcam, ab8878), or rabbit antibody to GFP (1:400, Life Technologies, A-6465). Sections were then washed and incubated at 4 °C with fluorochrome-conjugated secondary antibodies (1:1,000, Cy3-conjugated donkey anti-mouse IgG, Jackson Immuno Research; 1:1,000, Cy5-conjugated donkey anti-rabbit IgG, Jackson Immuno Research; or 1:2,000 donkey anti-rat IgG Alexa Fluor 555, Abcam, ab150154). Images were taken using a Nikon Eclipse Ti C1SI Spectral Confocal microscope and a Nikon A1R Multiphoton microscope. Quantification was performed using ImageJ (NIH) by an experimenter blind to genotype and/or drug treatment.

cFos immunolabeling. Mouse spinal cord tissue was isolated and sectioned as described above. Free-floating spinal cord sections were blocked for 10 min with 0.3% H_2O_2 and then for 5 min with 1% NaBH₄. Sections were incubated overnight at 4 °C with rabbit antibody to cFos (1:5,000, Abcam, ab7963). Sections were washed and incubated for 2 h in biotinylated anti-rabbit secondary antibody (1:1,000; Vector Laboratories) then processed with Vectastain ABC kit (Vector Laboratories) and developed for 1 min using 3,3-diaminobenzidine with nickel. Images were taken using an Olympus Virtual Slide System Macro

Slide Scanner and number of Fos-immunoreactive cells within the superficial spinal dorsal horn were counted. Imaging and quantification were performed by an experimenter blind to genotype and drug treatment.

***Ex vivo* spinal cord recordings.** Electrically evoked field potentials in the superficial dorsal horn were recorded as previously described[15]. Briefly, animals were anesthetized with urethane (2 g/kg) and perfused transcardially with an ice-cold oxygenated (95% O_2, 5% CO_2) sucrose-based artificial cerebrospinal fluid (S-aCSF) solution containing the following (in mM): 252 sucrose, 2.5 KCl, 6 $MgCl_2$, 1.5 $CaCl_2$, 1.25 NaH_2PO_4, 26 $NaHCO_3$, 4 kynurenic acid and 10 D-glucose. The lumbar spinal column was rapidly removed and immersed in ice-cold S-aCSF, and the spinal cord was obtained by laminectomy. Spinal cord explants were allowed to recover for 60 min in an immersion chamber containing oxygenated (95% O_2, 5% CO_2) aCSF (in nM: 126 NaCl, 2.5 KCl, 2 $MgCl_2$, 2 $CaCl_2$, 1.25 NaH_2PO_4, 26 $NaHCO_3$ and 10 D-glucose) at room temperature. Post-synaptic field potentials (fPSPs) were recorded via a borosilicate glass electrode inserted into the dorsal side of the spinal cord explant in the dorsal root entry zone. Electrodes were inserted superficially to a depth of no more than 125 μm from the dorsal surface of the spinal cord measured with an MPC-285 manipulator with MPC-200 controller (Sutter Instrument Company). Electrodes had a tip resistance of 3–4 MΩ when filled with aCSF. fPSPs were evoked by electrical stimulation of the dorsal root using an aCSF-filled borosilicate suction electrode placed near the cut end of the dorsal root. Field potentials were amplified with a multiclamp 700B amplifier (Molecular Devices), digitized with a Digidata 1322A (Molecular Devices) and recorded using pClamp 10 software (Molecular Devices). Data were filtered during acquisition with a low-pass filter set at 1.6 kHz and sampled at 10 kHz. Test stimuli were presented every 60 s to evoke fPSPs, and baseline was determined as a 30-min period of stable responses (less than 15% variability). After a stable baseline was observed, naloxone (10 μM) was applied via bath or LTP was evoked by stimulation at 2 Hz for 2 min with a 25% higher intensity than baseline stimulation, after which stimulation intensity was returned to baseline levels and test pulses were again delivered once per minute. Data were analyzed using ClampFit 10 software (Molecular Devices). The area of fPSPs relative to baseline was measured from 0 to 800 ms after the onset of the fPSP.

Statistics. All data are presented as mean ± s.e.m., and each data point represents an individual animal or experiment. Tests of statistical difference were performed with GraphPad Prism 6 software using unpaired *t*-test (two-sided), or ordinary one-way ANOVA with *post hoc* Bonferroni or Sidak's test. Time course and daily anti-nociception experiments were analyzed using a two-way repeated measure ANOVA with *post hoc* Sidak test. Sample sizes are consistent with those reported in similar studies and provide sufficient power to detect changes with the appropriate statistical analysis. Data used for statistical comparison fit a Gaussian distribution, and variances were equivalent between groups. For all experiments, a criterion α level was set at 0.05.

28. Trang, T., Ma, W., Chabot, J.-G., Quirion, R. & Jhamandas, K. Spinal modulation of calcitonin gene–related peptide by endocannabinoids in the development of opioid physical dependence. *Pain* **126**, 256–271 (2006).
29. Ferrini, F. *et al*. Morphine hyperalgesia gated through microglia-mediated disruption of neuronal Cl⁻ homeostasis. *Nat. Neurosci.* **16**, 183–192 (2013).
30. Ichikizaki, K., Toya, S. & Hoshino, T. A new procedure for lumbar puncture in the mouse (intrathecal injection) preliminary report. *Keio J. Med.* **28**, 165–171 (1979).
31. Oyebamiji, A.I. *et al*. Characterization of migration parameters on peripheral and central nervous system T cells following treatment of experimental allergic encephalomyelitis with CRYAB. *J. Neuroimmunol.* **259**, 66–74 (2013).
32. Trang, T., Beggs, S., Wan, X. & Salter, M.W. P2X4-receptor-mediated synthesis and release of brain-derived neurotrophic factor in microglia is dependent on calcium and p38-mitogen-activated protein kinase activation. *J. Neurosci.* **29**, 3518–3528 (2009).
33. Weilinger, N.L., Tang, P.L. & Thompson, R.J. Anoxia-induced NMDA receptor activation opens pannexin channels via Src family kinases. *J. Neurosci.* **32**, 12579–12588 (2012).